Ambient and laboratory evaluation of a low-cost particulate matter sensor☆

K.E. Kelly [a, *], J. Whitaker [b], A. Petty [a], C. Widmer [a], A. Dybwad [c], D. Sleeth [d], R. Martin [e], A. Butterfield [a]

[a] University of Utah, Department of Chemical Engineering, 3290 MEB, 50 S. Central Campus Dr., Salt Lake City, UT, United States
[b] University of Utah, Department of Electrical and Computer Engineering, 2110 MEB, 50 S. Central Campus Dr., Salt Lake City, UT, United States
[c] PurpleAir, 15183 Moab Way, Draper, UT, United States
[d] University of Utah, Rocky Mountain Center for Occupational and Environmental Health, 391 Chipeta Way, Suite C, Salt Lake City, UT 84108, United States
[e] Utah State University, Department of Civil and Environmental Engineering, Utah Water Research Laboratory, 8200 Canyon Road, Logan, UT 84322, United States

ARTICLE INFO

ABSTRACT

Low-cost, light-scattering-based particulate matter (PM) sensors are becoming more widely available and are being increasingly deployed in ambient and indoor environments because of their low cost and ability to provide high spatial and temporal resolution PM information. Researchers have begun to evaluate some of these sensors under laboratory and environmental conditions. In this study, a low-cost, particulate matter sensor (Plantower PMS 1003/3003) used by a community air-quality network is evaluated in a controlled wind-tunnel environment and in the ambient environment during several winter-time, cold-pool events that are associated with high ambient levels of PM. In the wind-tunnel, the PMS sensor performance is compared to two research-grade, light-scattering instruments, and in the ambient tests, the sensor performance is compared to two federal equivalent (one tapered element oscillating microbalance and one beta attenuation monitor) and gravimetric federal reference methods (FEMs/FRMs) as well as one research-grade instrument (GRIMM). The PMS sensor response correlates well with research-grade instruments in the wind-tunnel tests, and its response is linear over the concentration range tested (200–850 $\mu g/m^3$). In the ambient tests, this PM sensor correlates better with gravimetric methods than previous studies with correlation coefficients of 0.88. However additional measurements under a variety of ambient conditions are needed. Although the PMS sensor correlated as well as the research-grade instrument to the FRM/FEMs in ambient conditions, its response varies with particle properties to a much greater degree than the research-grade instrument. In addition, the PMS sensors overestimate ambient PM concentrations and begin to exhibit a non-linear response when $PM_{2.5}$ concentrations exceed 40 $\mu g/m^3$. These results have important implications for communicating results from low-cost sensor networks, and they highlight the importance of using an appropriate correction factor for the target environmental conditions if the user wants to compare the results to FEM/FRMs.

© 2016 Elsevier Ltd. All rights reserved.

1. Introduction

Particulate matter (PM) concentration is a key metric for air quality because of its adverse effects on human health, visibility, and climate. From the health standpoint, elevated PM levels are associated with numerous adverse effects including cardiac arrhythmia, lung cancer, heart disease, and mortality (Brook et al., 2010; Lepeule et al., 2012; Peters et al., 2000; Pope et al., 2011). Air pollution accounted for 7 million deaths worldwide in 2012 with fine particulate matter ($PM_{2.5}$) being the greatest contributor (World Health Organization, 2014). Because of these health and environmental impacts, the US EPA (United States Environmental Protection Agency) regulates ambient concentrations of PM with an aerodynamic diameter of 2.5 μm and smaller ($PM_{2.5}$) and of PM with an aerodynamic diameter of 10 μm and smaller (PM_{10}). Compliance with these standards is based on a federal reference method (FRM), which involves collecting PM in the appropriate size

---

☆ This paper has been recommended for acceptance by Charles Wong.
* Corresponding author.
E-mail address: kerry.kelly@utah.edu (K.E. Kelly).

range on a filter, to determine the 24-h PM concentration and annual average of these PM concentrations. In addition, the EPA has approved federal-equivalent methods (FEMs) for measuring PM concentrations, and this type of monitoring equipment can provide PM concentrations at hourly intervals. Rather than using direct gravimetric measures like FRMs, PM FEMs use alternative methods, such as optical, beta ray attenuation, or tapered element oscillation, to determine PM concentration. Government agencies collect PM concentrations from sparsely distributed monitoring stations equipped with high-quality, expensive FRM/FEMs for their planning, public outreach and forecasting. However, these sparsely distributed stations may not accurately represent the pollutant gradients within a city (Bell et al., 2011; Steinle et al., 2013), particularly for traffic-related air pollutants such as $PM_{2.5}$ (Health Effects Institute, 2010). Consequently, this poor spatiotemporal resolution of PM levels inhibits estimates of personal PM exposure and epidemiologic studies of PM's health effects, validation of emission inventories and air-quality models, and an understanding of the efficacy of emission-reduction policies (EPA, 2009).

Low-cost sensors offer the potential for gathering large quantities of high-resolution, air-quality data, but the performance of these sensors has not been thoroughly evaluated (Lewis, 2016). A few low-cost PM sensors have been evaluated in some field (Gao et al., 2015; Holstius et al., 2014; SCAQMD, 2016; Wang et al., 2015) and laboratory settings (Austin et al., 2015; Wang et al., 2015). These studies revealed that these PM sensors show promise. Wang et al. (2015) performed controlled laboratory studies of three low-cost sensors (Shinyei PPD42NS, Samyoung DSM501A, and Sharp GP2Y1010AU0F) and found that the PM measurements from these sensors generally correlated linearly ($R^2 = 0.89$) compared to research-grade instruments (TSI SidePak AM510 and a TSI a scanning mobility particle sizer over a particle concentration range of 0–1000 $\mu g/m^3$. Austin et al. (2015) also performed laboratory tests and found a linear correlation ($R^2 = 0.66$–0.99) for the Shinyei compared to a TSI Corp. aerosol particle sizer (APS) over the concentration range of 1–50 $\mu g/m^3$ although the slope of the linear relationship varied by more than a factor of 10 depending on the particle diameter. In the field, Gao et al. (2015) compared the response of the Shinyei sensor in a polluted region of China (24-h $PM_{2.5}$ 330–413 $\mu g/m^3$) and found correlations to co-located research-grade instruments ($R^2 = 0.86$–0.89) and gravimetric measures ($R^2 = 0.53$) in a 4-day study. Holstius et al. (2014) compared the performance of the Shinyei sensor to 24-h FEM ($R^2 = 0.72$, 3.5-month period) and research-grade measurements ($R^2 = 0.9$–0.94, 7-day period) in Oakland, CA with $PM_{2.5}$ concentrations ranging from 2 to 21 $\mu g/m^3$. The South Coast Air Quality Management District (SCAQMD) recently released a draft report comparing the PurpleAir (Plantower PMS 1003) sensors to two FEMs (beta attenuation monitor, BAM and GRIMM FEM) over a two-month period in Riverside, CA (24-h $PM_{2.5}$ 2–40 $\mu g/m^3$) and found good correlations ($R^2 > 0.9$, 24-h average FEM measurements) (SCAQMD, 2016).

As noted in several of the studies, these low-cost sensors have drawbacks. They are not as accurate or precise as FEMs (Isaac, 2014). Some have limited sensitivity and can be affected by humidity and other factors, and sets of the same sensors can perform inconsistently (Gao et al., 2015; Wang et al., 2015). Low-cost, gas-phase sensors can experience significant sensor drift (Piedrahita et al., 2014). Many of these sensors lack independently gathered calibration data under conditions for which they are deployed, quality assurance procedures, or descriptions of when the sensors may provide inaccurate readings. In spite of these potential challenges, organizations have been collecting and posting PM concentrations online and even posting air-quality indices based on these data. (Bischoff, n.d.; PurpleAir, 2016). Presenting information

from these PM sensors can cause either unnecessary public concern or complacency about pollution levels and the associated health risks (Isaac, 2014).

Consequently, there is a need for improved low-cost PM sensors and to validate sensors under real-world as well as laboratory conditions. This paper focuses on evaluating a relatively new PM sensor, the Plantower PMS 1003/3003, in an ambient environment during periodic episodes of high PM levels and in a laboratory wind tunnel. Elevated PM levels are a particularly important issue in northern Utah, which is classified as nonattainment for the 24-hr $PM_{2.5}$ national ambient air quality standard (NAAQS). During winter, atmospheric stability and the mountainous topography result in cold-air pools (CAPs), which trap pollutants, and during these CAPs maximum daily average $PM_{2.5}$ concentrations can reach double the national ambient air quality standard of 35 $\mu g/m^3$. Although PM concentrations in northern Utah have declined over the past 40 years due to the implementation of air-quality regulations, Salt Lake County in northern Utah typically exceeds for 24-hr $PM_{2.5}$ levels on 18 days per year, and these exceedances almost exclusively occur during winter-time CAPs (Whiteman et al., 2014). During these CAPs in northern Utah, $PM_{2.5}$ levels tend to increase at a rate of approximately 10 $\mu g/m^3$ per day until reaching a plateau (typically 60–100 $\mu g/m^3$, depending on the location). CAPs are associated with temperatures below 0 $^\circ$C, relative humidity (RH) in excess of 50% and light wind speeds (Whiteman et al., 2014). These episodes of poor air quality create significant health and quality-of-life concerns for the region's citizens, including increased incidence of asthma, juvenile arthritis, pre-term birth and mortality (Beard et al., 2012; Pope et al., 2002; Zeft et al., 2009). As a result of similar topographies and weather patterns, California's San Joaquin Valley, Beijing, Mexico City, and Tehran also experience similar events with accompanied high levels of fine PM (Afsarmanesh, 2013; Molina et al., 2007; Watson and Chow, 2002; Zhang and Cao, 2015).

As a result of public concerns, a local community organization, PurpleAir (PurpleAir, 2016), developed a network of 120 low-cost air-quality measurement devices based on the PMS sensor and is posting values online. However, the performance of these sensors has not been thoroughly evaluated, particularly under the atmospheric conditions for which they are being deployed. Furthermore, the public does not understand the differences between values posted by the low-cost sensors compared to FEMs/FRMs. This study partnered with the local community organization to evaluate PMS sensor performance in a laboratory setting and under realistic ambient conditions during several CAPs, when public interest in PM levels is high, and during several clean-air periods. The ultimate goal is to lead to a better understanding of PMS sensor performance and to develop recommendations for when and how the sensor results may be comparable to FEM/FRMs.

2. Material and methods

This study evaluated the Plantower PMS 1003/3003 laser particle counter in a wind tunnel and outdoors during several winter CAP events. The PMS 1003/3003 is a relatively inexpensive ($35), commercially available particle sensor (Fig. 1). It employs a fan to draw air through a chamber where it is exposed to a laser-induced light, and 90° scattered light is detected by a photo-diode detector. The laser wavelength was not available from the manufacturer, but it was estimated at 650 $\pm$ 10 nm with a Lambda 35 spectrophotometer (PerkinElmer, Inc.). The back of the chamber contains a light-trap to prevent spurious scattering of laser light. Light scattering is converted into PM_1, $PM_{2.5}$ and PM_{10} concentrations. According to the manufacturer, it detects PM in the range of 0.3 μm to 10 μm, and it has a 10-s response time. The majority of the outdoor
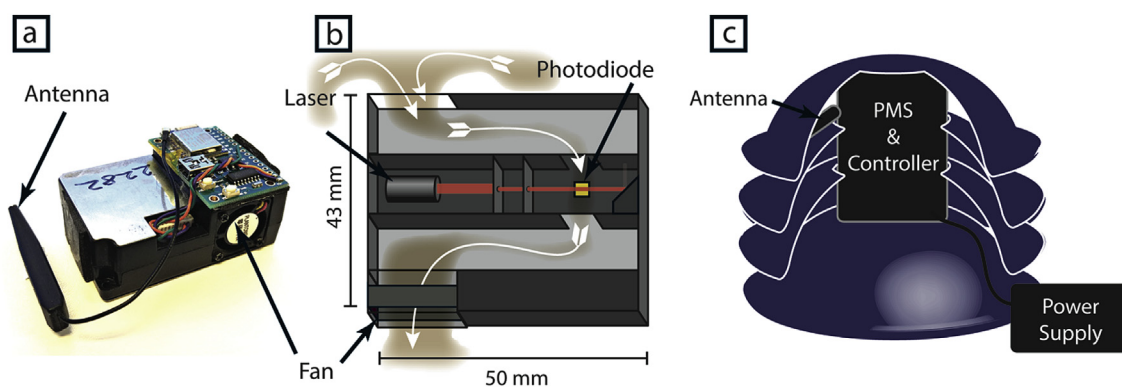
Fig. 1. (a) Plantower PMS 3003 (b) schematic of the Plantower PMS 3003 sensor, and (c) housing for the outdoor PMS sensor.

samples were collected with the PMS 1003, but during the course of the study, Plantower released a new model, PMS 3003, and limited measures were collected with the PMS 3003 because the outdoor housing for the AirU-PMS 3003 was not complete. The wind-tunnel tests were performed with both the 1003 and the 3003 models. The PMS 1003/3003 sensor generates PM_1, $PM_{2.5}$ and PM_{10} mass concentration estimates, either without a correction factor (called CF = 1) or using their atmospheric calibration factor (called CF = atmos). The manufacturer does not provide details on what this calibration factor is or how it was developed. The PMS 1003 also reports particle counts in five bins with mean sizes of 0.3, 0.5, 1, 2.5, 5, and 10 μm.

The sensor network operated by a local community organization, PurpleAir, is based on an ESP8266 WiFi chip and the PMS 1003 sensor. Each sensor is integrated with a wireless antenna and runs custom Arduino firmware. The firmware receives values from the PMS 1003 every second and averages these over 20 s before transmitting data wirelessly to an online database. All time stamps for PurpleAir data are server time because the data are transmitted live and not stored on the sensor. The PurpleAir PMS 1003 sensor is 5.5 × 4 × 2.5 cm, and conservatively it draws 3 W of power, including the wireless signal.

The PMS 3003 was integrated into a package (dubbed AirU) along with a PMS 3003, a Bosch BMP180 (for temperature, pressure, altitude), a SGX Sensor Tech MiCS-4514 (for CO, NO2), an Aosong Electronics DHT22 (for temperature and humidity), and an Adafruit Ultimate GPS chip were integrated into a small custom printed circuit board, which interfaced with a Beaglebone Black. AirU reports 1-min average readings and has the capability of storing 550 MB of data (lab mode) or uploading it directly to a web interface (field mode). In field mode, each set of measurements is written to a SQLite database on the AirU station, and the measurements are uploaded to a central custom web-based database. Because the PMS 3003 sensor became available during the course of the study, AirU stations were under development and the outdoor housing was not complete, they were deployed in the wind-tunnel experiments and periodically, weather permitting, in the outdoor settings. AirU's dimensions are 84 × 49 × 25 cm. It requires a 5 V power supply, and conservatively it draws 2W of power.

In addition, two Shinyei PPD42NS sensors were deployed in the wind-tunnel experiments. These were integrated with an Arduino Uno board and communicated their results (lo-pulse occupancy) directly through USB to a computer using the Arduino environment. The Shinyei uses an infrared light-emitting diode (IRED) as its light source and captures light scattering in the 45° degree forward-scattering direction with a photodiode. The raw sensor signal consists of low pulse occupancy (fraction of time when the digital signal is low), which is proportional to particle count concentration. As described by Gao et al. (2015), for outdoor ambient

monitoring the sensor's raw signal must to be calibrated with co-located reference instruments to obtain mass concentration measurements (i.e., Holstius et al., 2014).

2.1. Limit of detection (LOD)

We estimated the limit of detection for the PMS 1003 using the method of Kaiser and Specker (1956).

$$LOD = 3\sigma_{blk}/k$$

where,

σ_{blk} is the standard deviation at blank conditions maintained by filling the chamber with air cleaned by high-efficiency particulate air (HEPA) filters.

k is the slope of the fitted line obtained from linearity experiments (two slopes from laboratory wind-tunnel and the other from the ambient measurements).

For the laboratory experiments, σ_{blk} is calculated over a measurement time of 90 min and 197 sensor readings from two different sensors. For the ambient experiments, σ_{blk} is calculated for all readings when either co-located FEM valid hourly reading was below 1 μg/m^3 (28 readings).

2.2. Ambient tests

The PMS sensors are compared to two FEMs, one GRIMM model 1.109 and $PM_{2.5}$ and PM_{10} gravimetric measurements (FRMs) at a state monitoring site located at the Hawthorne Elementary School in the southeast region of Salt Lake City in Salt Lake County, UT (USEPA, 1999). The Hawthorne monitoring station (AQS: 49-035-3006) is located in an urban residential area (Lat: 40.7343, Long: −111.8721) at an elevation of 1312 m. This site was established to represent population exposure in the Salt Lake City area. This is the controlling monitoring station for the Salt Lake County $PM_{2.5}$ non-attainment area, meaning that this station has, on-average, the highest state-monitored $PM_{2.5}$ levels in county. The study site lies 3.3 km south and east of the Salt Lake City Center. Salt Lake City has 190,000 residents, and it lies in the center of Utah's Wasatch Front (population: 2,217,304, US Department of Commerce, 2010). This contiguous chain of cities and towns is growing rapidly and expected to add 1.5 million residents by 2040 (Brookings Institute, 2012). The Wasatch Front is a long and narrow valley, approximately 130 km long and 8 km wide, on average. It is bordered by the Wasatch Mountains (3620 m) to the east and Utah Lake, the Oquirrh Mountains (3237 m), and the Great Salt Lake to the west.

This station's standard measurements include a Thermo Scientific 1405-F tapered element oscillating microbalance (TEOM) Filter

Dynamics Measurement Systems Monitor (FEM, hourly $PM_{2.5}$ and PM_{10}), Thermo Scientific Sharp 5030 BAM (FEM, hourly $PM_{2.5}$), temperature, RH, and solar radiation as well as gas-phase criteria pollutants. The cost of these instruments range from $20,000 - $30,000, depending on the configuration and required accessories. The TEOM employs a size-selective inlet and contains a filter mounted on the tip of a hollow glass tube. When particles deposit on the filter, the oscillation frequency of the tube changes proportionally to the PM mass on the filter (Kulkarni et al., 2011). The Sharp also employs a size-selective inlet but collects PM on a tape. It measures the attenuation of beta radiation, which is proportional to particle mass (Kulkarni et al., 2011). The GRIMM 1.109 uses light scattering to estimate PM mass concentration and count over the size range of 0.25–32 μm in 31 size classes. It draws air into a detection region where particles are illuminated by a laser (655 nm); the scattered light is collected at approximately 90° by a mirror and transferred to a recipient diode. The diode signals are converted to a pulse height and then classified by size and count. These counts are converted every 6 s to a mass distribution (Peters et al., 2006).

As available, data from a collocated TSI Aerodynamic Particle Sizer (APS), model 3321, was also used for size distribution comparisons. The APS uses two partially overlapping laser beams to detect time-of-flight measurements of accelerated particles and thereby records the aerodynamic diameters of the target particles. The APS collects number counts ($\#/cm^3$) into 52, logarithmically spaced size bins from <0.523 μm to 19.81 μm in aerodynamic diameter. Further, the instrument reports a lower channel bound of 0.487 μm. It should be noted that as described by Murphy et al. (2004) and others, the reported aerodynamic diameters are nominally related to the GRIMM reported optical or physical diameters by a multiplier of the square root of the particle density or specific gravity ($d_{aero} = d_{phys} \rho^{0.5}$). Consequently for the same particle, the APS may report a larger particle diameter (aerodynamic) than the optical instrument.

During the course of the study (January 6–February 17, 2016) the average temperature was 0.0 °C (range: −8.9–15.9 °C) and the RH was 69.8% (range: 26.6–88.6%). Previous studies for this station during winter indicate that $PM_{2.5}$ is comprised of approximately 65% secondary inorganic aerosols (ammonium chloride, ammonium nitrate, and ammonium sulfate), 20% organic carbon, 3% elemental carbon, 3% crustal material, and 9% other) with source contributions from gasoline combustion, wood burning/cooking, diesel combustion, and crustal/re-entrained road dust (DAQ (Utah Division of Air Quality), 2013; Kelly et al., 2013).

2.3. Wind-tunnel tests

Laboratory studies were performed in a low-speed wind tunnel (Schmees et al., 2008) operated at a wind-speed of 0.5 m/s (Fig. S-1). The tunnel has an associated air compressor, a dry-dust generator (SAG 410, Topas Gmbh, Dresden, Germany) and an aerosol dispersion system, which employs a dual tracking system with an injection nozzle mounted on a motor allowing the nozzle to move vertically in a reciprocating motion. The motor in turn is mounted on an overhead tracking system that conveyed the nozzle laterally backwards and forwards. The dry dust is alumina oxide with a mass median diameter of 4.9 ± 1.7 μm and a density of 4.0 g/cm^3 (Duralum, Washington Mills, Niagara Falls, NY, USA). Two PMS 3003s and two PMS 1003s were compared to one GRIMM model 1.109 (same instrument as the ambient tests) and one TSI DustTrack II 8530. The $PM_{2.5}$ measurements from the DustTrack were corrected for mass concentration using an AirMetrics MiniVol filter that was collected for each day of wind-tunnel sampling, during the approximately 6-h test.

In the wind-tunnel experiments, one of five particle injection rates (0.2, 0.5, 0.8, 1 g/hr) was selected, and the injection rate was held constant for 30 min. Immediately after the injection rate was changed, particle concentrations fluctuate and reach steady state in 3–5 min. Particle injection varied in the horizontal and vertical direction on a time-scale of approximately 1 min as the injector moves across the diffuser, causing a corresponding variation in PM concentration depending on the precise location of each sensor in the wind tunnel. Consequently, sensor performance was compared on 10-min averages.

## 3. Results and discussion

3.1. Limit of detection

The PMS 1003 LOD ranges from less than 1–3.22 μg/m^3 under laboratory conditions to 10.5 μg/m^3 under ambient conditions (details in Tables S-1). This is in the range of published laboratory estimates of LOD for PM low-cost sensors − less than 1–26.9 μg/m^3 in laboratory settings (Austin et al., 2015; Wang et al., 2015). During the ambient study period, only 28 hourly FEM readings were less than 1 μg/m^3, and additional data may help refine the estimated ambient LOD.

3.2. Ambient results

Tables S-2 shows the meteorological conditions during the ambient measurements. Figs. 2 and 3 compare the PMS, GRIMM and FEM measurements. It clearly shows that the PMS sensors follow the $PM_{2.5}$ concentration trends of the two co-located FEM monitors during the build up and dissipation of several CAPs during the winter of 2016. This type of PM concentration trend is typical of winter CAPs forming and disbursing in the Salt Lake Valley (Whiteman et al., 2014). During this study, FEM-measured hourly $PM_{2.5}$ concentrations averaged 17.5–20.1 μg/m^3 (range: 0–70.6 μg/m^3). Fig. 3 also shows that the two PMS sensors are highly correlated with each other ($R^2 > 0.99$) and that the PMS sensors overestimate $PM_{2.5}$ concentrations when $PM_{2.5}$ levels exceed 10 μg/m^3.
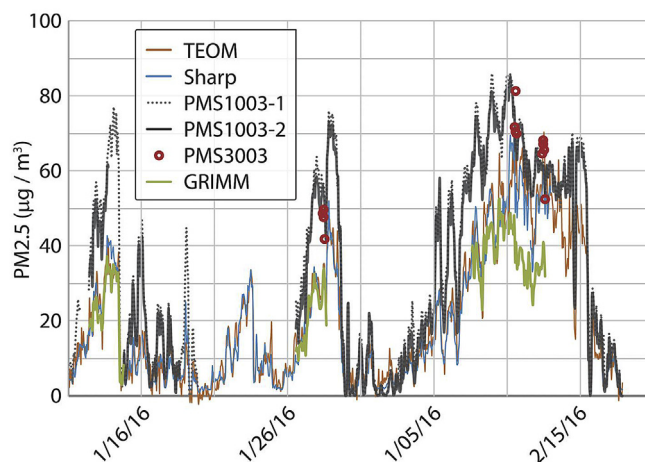
Fig. 2. Comparison of co-located hourly $PM_{2.5}$ (μg/m^3) concentrations from the Utah Division of air quality monitors (DAQ TEOM, DAQ Sharp), a research grade monitor (GRIMM), and the PMS sensors from January 11, 2016 to February 17, 2016. Note the PMS sensors went offline between January 20 and January 27th because of power-supply problems. This caused the PMS1003-1 and PMS1003-2 data to be 81% and 74% complete, respectively.
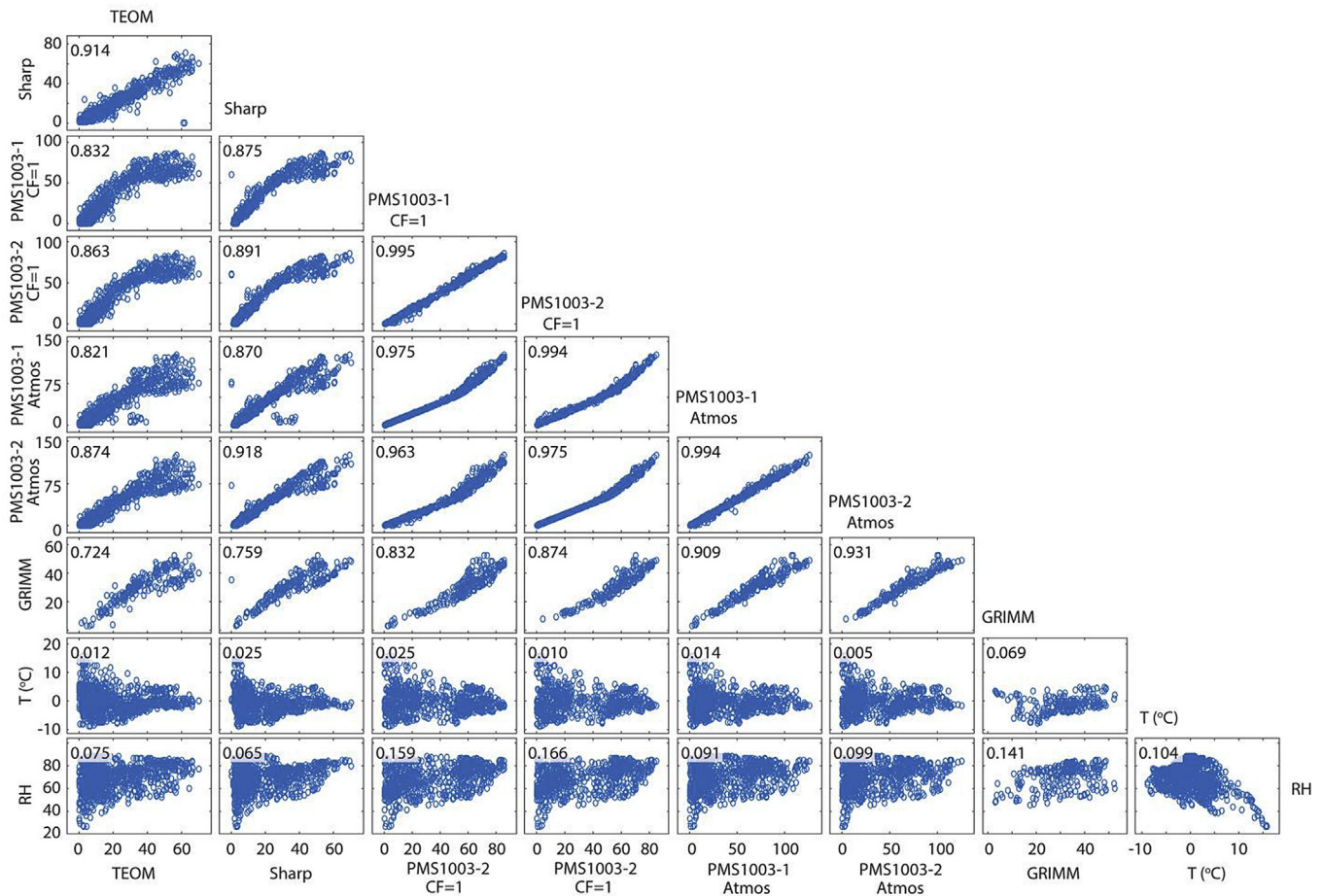
Fig. 3. Scatter plots and correlation coefficients for $PM_{2.5}$ (µg/m³) concentrations (PMS 1003-1/2) with FEMs (TEOM and Sharp), research-grade monitor (GRIMM), temperature and RH. No correlation was seen between $PM_{2.5}$ concentration measured between any of the devices and wind speed (R^2 of 0.03−0.04), results not shown.

3.2.1. 24-Hour results

Compliance with the NAAQS is based on 24-h PM mass concentrations, and Table 1 shows the correlation coefficients between the various measurements and 24-h average PM mass concentrations. Both of the FEM instruments correlate with the 24-h $PM_{2.5}$ mass measurements with an $R^2 > 0.99$. The PMS $PM_{2.5}$ concentrations are also well correlated with the 24-h mass average concentration ($R^2 > 0.88$), which is slightly better than the GRIMM research-grade instrument ($R^2 = 0.79$) although this instrument had fewer observations. The PMS-gravimetric correlation is also better than the Shinyei correlations to 24-h gravimetric measures reported by Gao et al. ($R^2 = 0.53$), although their observation period was four 4 days (8 locations) and their 24-h average $PM_{2.5}$ concentrations were much higher (330−413 µg/m³) than this study. The SCAQMD recently published preliminary comparisons of the $PM_{2.5}$ measurements from three PMS 1003s and two FEMs, with

high correlations ($R^2 > 0.9$) over a 2-month period. Holstius et al. (2014) also report 24-h comparisons of the Shinyei sensor with FEM measurements ranging from 2 to 25 µg/m³, over a 3.5-month time period (R^2 of 0.72). This lower correlation for the Shinyei may be due to the relatively low $PM_{2.5}$ concentrations present during this study and the low sensitivity of Shinyei (as well as other sensors) at these low concentrations. It should be noted that neither the SQAMD or the Holstius used gravimetric comparisons. It is also interesting to note that the PMS PM_{10} concentration correlates slightly better with the 24-h $PM_{2.5}$ mass concentration than the PMS $PM_{2.5}$ concentration; however, the SQAMD reported that the PMS 1003 PM_{10} measurements did not correlate well with FEM PM_{10} 24-h measurements ($R^2 = 0.34−0.45$). The reason for this better PM_{10} correlation in the Utah location is not completely clear. However, the configuration of the PMS sensor and the results suggest that the allocation of light scattering to PM_1, $PM_{2.5}$, and

Table 1
Coefficient of determination (R^2) between Utah DAQ 24-h $PM_{2.5}$ mass measurements (FRM) and 24-average concentration from the co-located measurement devices. Scatter plots for these correlations can be found in Fig. S-2 (supplementary material).

FRM	TEOM $PM_{2.5}$	Sharp $PM_{2.5}$	PMS PM_1	PMS $PM_{2.5}$	PMS PM_{10}	GRIMM $PM_{2.5}$	GRIMM PM_{10}
$PM_{2.5}$ mass	0.994	0.994	0.825, 0.825	0.884, 0.887	0.918, 0.920	0.793	0.732
[a]Obs	46	43	32, 33	32, 33	33, 32	12	12
PM_{10} mass	0.911	0.884	0.825, 0.875	0.860, 0.909	0.872, 0.924	0.782	0.752
[a]Obs	22	19	19,18	19,18	19,18	7	7

[a] Obs: number of observations that correspond to correlation coefficient in the row above. For the PMS sensors, the first number corresponds to Sensor 1, and the second number corresponds to Sensor 2.

PM_{10} is based on a theoretical model rather than a measurement. In Salt Lake City during the winter measurements, PM_{10} and $PM_{2.5}$ was highly correlated ($R^2 = 0.88–0.91$), and when $PM_{2.5}$ concentrations exceed 10 μg/m³, approximately 90% of the 24-h PM_{10} mass was $PM_{2.5}$ mass. In the SQAMD study in Riverside, CA, a smaller fraction of the 24-h PM_{10} mass was $PM_{2.5}$ mass.

There are a few potential reasons for the PMS's better response than the Shinyei in ambient studies: flow control into the sensor, the sensor light source, and intrinsic limitations in the comparison of gravimetric and optical estimates of PM concentration. The PMS employs a fan to draw air past the sensor, whereas the Shinyei uses resistive heating to induce convective flow past the sensor. Convective flow is proportional to the temperature gradient, which will vary with ambient temperature. One study reports a significant temperature effect for the Shinyei sensor during a winter-time evaluation ($-3.5–19.2$ °C) (Gao et al., 2015), while another study found no temperature association during a spring evaluation (20–30 °C) (Holstius et al., 2014). This difference in reported temperature effects could potentially be due to the difference in the temperature ranges or the difference in the concentration ranges between the two studies. The Shinyei uses an IRED as its light source and measures 45° forward light scattering, whereas the PMS uses a laser through a pinhole and measures 90° light scattering. This IRED is a much more diffuse light source than the PMS's laser-pinhole setup. Further the IREDs typically generate light with wavelengths between 870 and 980 nm (Schubert, 2006), and the PMS sensor estimated laser wavelength is estimated at 650 nm. Typically, lasers used for PM measurements have wavelengths between 450 and 700 nm (Chow et al., 2002). Finally, as discussed in detail by Holstius, there are limitations in comparing optical estimates of PM concentration to gravimetric measures due to differences in PM mass, size distribution, or optical properties, or a combination of these factors. Other studies tend to show better correlations between low-cost PM sensors and optical measurements compared to gravimetric measurements, or they tend to show better correlations under laboratory conditions (Austin et al., 2015; Gao et al., 2015; Wang et al., 2015).

3.2.2. Hourly results

For the same time period presented in Figs. 2 and 3 shows scatter plots of the relationship on an hourly basis between the PMS sensors, the FEMs, the GRIMM, temperature and RH. The FEMs correlate well with each other ($R^2 = 0.91$) and the PMS sensors also correlate well with each other ($R^2 > 0.97$ for the same setting $CF = 1$ or atmos). This good correlation between PMS units was also seen in the SQAMD study (SCAQMD, 2016). The PMS sensor ($CF = 1$) readings begin to exhibit a non-linear response when the FEMs reach approximately 40 μg/m³. Other studies also observed non-linear responses for low-cost sensors, particularly for particles with small diameters and for ammonium nitrate particles (Austin et al., 2015; Wang et al., 2015). At this same concentration of 40 μg/m³, the PMS ($CF = 1$) and PMS (atmos) readings begin to diverge, suggesting that the PMS (atmos) values include some correction for this non-linear behavior. Just as with the gravimetric measurements, the PMS sensors correlate slightly better than the GRIMM to $PM_{2.5}$ FEM hourly measures (R^2 of $0.83–0.92$ vs. $0.72–0.76$) although the GRIMM had fewer measurements. During the study period, the FEMs, the PMSs, and the GRIMM showed no correlation between temperature and hourly PM levels. The FEMs show no/limited correlations between RH and PM concentrations ($R^2 = 0.07–0.08$), with the PMS and GRIMM correlations with RH being slightly higher ($R^2 = 0.09–0.17$). The FEMs have a conditioning unit to reduce humidity effects, and there is a natural correlation between wintertime CAPs and increased RH, so it may be difficult to resolve confounding effects of RH.

The stability of the PMS sensor response was also evaluated by considering how the normalized residuals changed over the course of the study. The normalized residuals were given by:

$$R_{es} = \frac{PM_{2.5,\ TEOM} - PM_{2.5,\ PMS}}{PM_{2.5,\ TEOM}}$$

where, R_{es} is the normalized residual, $PM_{2.5,TEOM}$ is the corrected TEOM hourly concentration (corrected to ensure that the TEOM 24-h $PM_{2.5}$ concentration matched the FRM 24-h $PM_{2.5}$ concentration), and $PM_{2.5,PMS}$ is the PMS hourly mass concentration. Fig. S-3 shows that the normalized residuals decrease slightly for both PMS sensors over the course of the sampling period (42 days). This decrease is statistically significant as determined by a student's t-test at the 95% confidence level. Since the PMS sensors overestimate PM concentration during the ambient tests, the sensor response may decrease as dust deposits on the photo detector, thereby reducing the sensor response and the residual. However, a long CAP occurred (February 1–15th) at the end of the sampling period, and the residuals decrease at high PM concentrations. It is possible that this is the cause for the decrease in residuals. Consequently, longer term sampling would be necessary to evaluate stability more thoroughly.

3.2.3. Size distributions

The PMS appears to be the first low-cost sensor (cost < $50) to provide a particle size distribution, and its total daily particle counts correlate well with the GRIMM (R^2 of 0.88, hourly average for 11 days). However, the PMS sensors overestimate total daily average PM counts by a factor of $1.5–2.4$ compared to the GRIMM and by a factor of $3.5–9$ compared to the APS. Grouping the GRIMM's size bins into size ranges that were similar to the PMS (0.3, 0.5, 1, 2.5, 5, and 10 μm) shows that the PMS overestimates particle counts by a factor of ($1.1–1.9$) for the 0.3 μm bin and increasingly overestimates particle counts as particle size increases: for the largest size bin (10 μm) by a factor of $30–500$. However, the particle counts are low in the upper size bins (GRIMM and APS particle counts range from 0 to 12 particles/liter in the PM_{10} size bin).

The GRIMM's and the APS's average daily particle counts show differences in particle size distribution (PSD) on different days, likely associated with CAPs. For example, a CAP began on February 1, 2016, and PM levels increased through February 10 when a partial CAP breakup occurred (Fig. 3a). Fig. 4 shows that both the GRIMM and PMS detect increasing counts from February 7 through February 9th, but on February 10 and 11th, the GRIMM's PSD particle size mode shifts from a single mode at 0.265 μm to a bimodal distribution with the largest mode at 0.375 μm with a second mode at 0.54 μm. The overall shape of the PMS PSD remained constant over all days. Considering hourly averages, the GRIMM's PSD also exhibits more variation. Over the period when the PMS sensors and the GRIMM were co-located, 86% of the GRIMM's particles fell into the 0.3 μm size bin with a 13% standard deviation. During this same period, 75% of the PMSs' particles fell into the 0.3 μm size bin with and 1.5% standard deviation. Both the PMS and GRIMM provide particle size distributions based on light scattering and produce results based on optical particle sizes. The APS provides particle size distributions based on aerodynamic sizing and aerodynamic particle diameters. The APS provides particle counts that are $2–5$ times lower than the GRIMM and 3.5 to 9 times lower than the PMS. Peters et al. (2006) also reported systematic difference in particle counts between similar GRIMM and APS systems. In particular, Peters et al. (2006) showed the APS routinely underpredicts particle counts for diameters <0.7 μm for polydispersed test aerosols (Arizona road dust). This is consistent with the aerosol size distributions and compositions for the observed ambient PM (Kelly et al.,
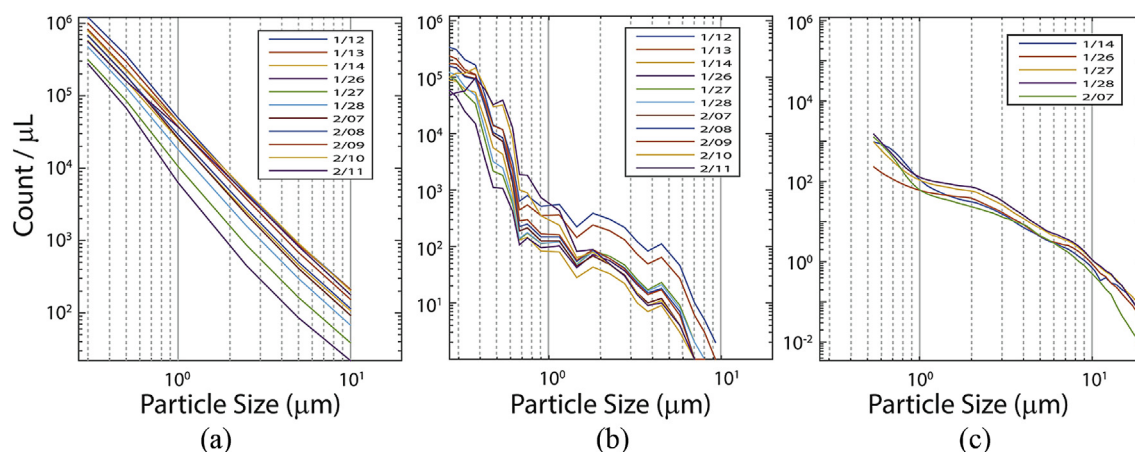
Fig. 4. Daily average particle counts for (a) the two PMS sensors, (b) the GRIMM and (c) the APS during ambient measurements at the Hawthorne monitoring station. Note that the x and y axes are log scale.

2013). Based on these results, it is likely that the size distribution provided by the PMS is based on theoretical model rather than a measurement.

The particle size distributions during CAPs may provide insight into the behavior of the PMS sensor. Both the PMS and GRIMM measure light scattering, and Mie scattering reaches its peak for particles with diameters in the range of 300−700 nm (wavelength of 400−700 nm) (Finlayson-Pitts and Pitts, 2000). During CAPs, particle mass distributions exhibit a peak in the range of 300−500 nm (Fig. S-4). We estimate laser wavelength of the PMS to be 650 nm. The GRIMM uses a laser with a wavelength of 655 nm, and the APS also uses a wavelength of 655 nm. It is possible that the difference in the sensor optics or the conversion of photodetector signal to PM concentration makes the PMS sensors apparently more responsive to CAP particles.

3.2.4. Model fit for hourly concentrations

We developed a model to fit the PMS (CF = 1) $PM_{2.5}$ response to the mass-adjusted TEOM measurement for the winter CAPS along the Wasatch Front, which was obtained by modifying the hourly TEOM measurements to achieve the same average as the 24-h gravimetric measurements. The TEOM was selected instead of the Sharp because it had more valid data points during the sampling period. We evaluated several types of models. The linear, linear below 40 $\mu g/m^3$, linear with humidity interaction, a 5th order polynomial, and an exponential fit provided the best fits. Temperature and precipitation did not significantly improve the model fit ($p < 0.001$). Although RH improved the linear model fit, it is naturally associated with higher PM levels during CAP events (R^2 0.07−0.08 for FEMs, which have sample conditioning systems). Tables S-3 shows the goodness of fit parameters for the best-fitting models. Of the fitting options, the exponential fit tends to have the best combination of goodness of fit, fewest parameters, smallest sum of squared errors, and normally distributed residuals. Fig. 5 shows the linear and exponential fits as well as the confidence intervals on the fit parameters. The figure also shows that the PMS sensor response is approximately linear up to 40 $\mu g/m^3$, and a linear fit for $PM_{2.5}$ concentrations below 40 $\mu g/m^3$ is a good model. Consequently, two fits are suggested for the study conditions:

$$PM_{2.5,\ PMS} = 1.81 \times PM_{2.5,TEOM} - 1.37 \left(\text{up to } 40 \ \mu g/m^3 \right)$$

$$PM_{2.5,\ PMS} = 90.9 \ e \left(-0.0333 \times PM_{2.5,TEOM} \right) - 7.16 (\text{full range})$$

Comparing the slopes for the PMS $PM_{2.5}$ sensor response during the winter-time CAPs in Utah to the SQAMD study for concentrations up to 40 $\mu g/m^3$ shows that the PMS's slope during CAPs is approximately 25% greater than for SQAMD study conditions. This difference in response may be due to the high scattering efficiency of particles during CAPs when particle composition is dominated by ammonium nitrate, ammonium sulfate and ammonium chloride (Kelly et al., 2013).

Fig. S-4 shows the scatterplot and linear relationship of the mass-adjusted hourly PM_{10} concentrations, and the suggested fit is given by:

$$PM_{10,PMS} = 1.15 \times PM_{10,TEOM} + 0.300 \ (\text{full range})$$

Where concentration is in $\mu g/m^3$.

Model fits where x = PMS and y = mass-adjusted TEOM are available in the supplementary material.

Other studies have proposed different fits for low-cost PM sensors under ambient conditions. Gao et al.[11] identified a 5th-order polynomial as the best fit for the Shinyei response to $PM_{2.5}$ levels measured by a DustTrack (R^2 0.91−0.94) under polluted atmospheric conditions (24-h $PM_{2.5}$ 330−413 $\mu g/m^3$) over a 4-day period. Holstius et al. (2014) identified a linear model as the best fit for the Shinyei sensor response to $PM_{2.5}$ levels measured by a 24-h FEM ($R^2 = 0.72$, 3.5-month period) in Oakland, CA with $PM_{2.5}$ concentrations ranging from 2 to 21 $\mu g/m^3$. These different fits for the same type of sensor under ambient conditions could result from differences in meteorological conditions during the two studies, the dramatically different PM levels, or differences in comparison metrics (light-scattering-based DustTrack vs. FEM). The differences in model choice support the challenges discussed by Gao et al. (2015) that the same model may not be a good fit for different locations or different conditions.

3.3. Wind tunnel evaluation

Table 2 shows the correlations between different sensors for the wind-tunnel tests. As discussed in the methods section, PM concentrations vary over the course of 1 min in any one location, so the comparisons are made on 10-min averages. Table 2 shows strong correlations between the same types of sensors (R^2 for PMS-PMS: 0.82 to 0.99 and for Shinyei-Shinyei: 0.72 to 0.95). The mass-adjusted DustTrack measurements are highly correlated with GRIMM ($R^2 = 0.8$−0.97) and the PMS sensors ($R^2 = 0.83$−0.98) but moderately correlated with the Shinyei ($R^2 = 0.59$−0.8). All sensors exhibited a linear response (Fig. 6) over the concentration range of 200−850 $\mu g/m^3$.
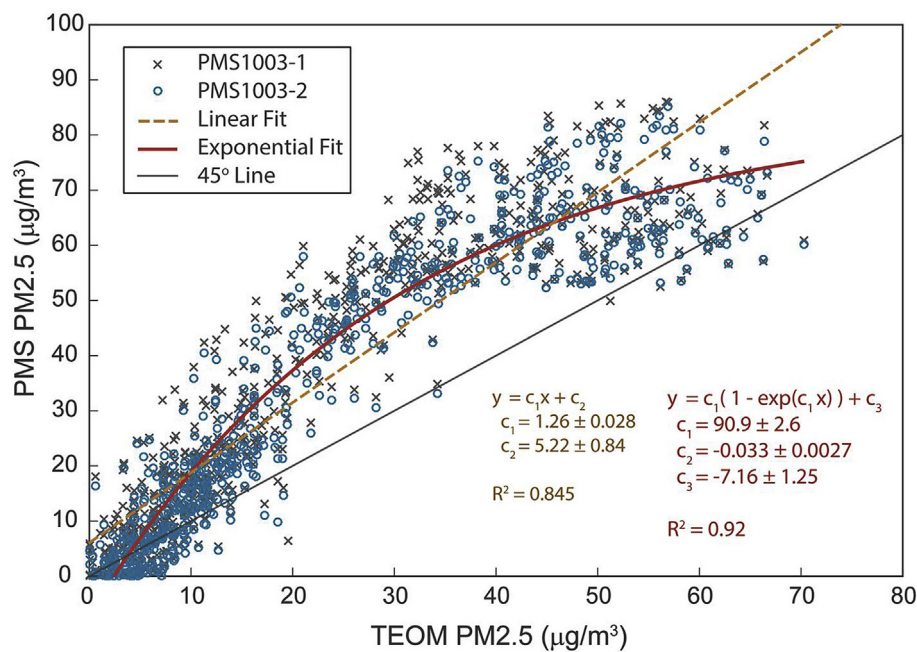
Fig. 5. Exponential and linear fit for the PMS sensor PM$_{2.5}$ concentrations.

3.3.1. Effect of housing

The original design of the PurpleAir outdoor housing appears to inhibit the ability of particles to flow into the PMS sensors in the wind-tunnel tests (particle mass median diameter of 4.9 μm, manufacturer). Fig. 6 compares PMS PM$_{2.5}$ concentrations with and without a housing with DustTrack PM$_{2.5}$ concentrations (mass adjusted). The PMS sensors without a housing are more responsive to changes in PM$_{2.5}$ concentration. Comparing the slopes of PMS sensors over time with and without housing on a 1-min average basis reveals a statistically significant difference between the slopes, at a 95% confidence level when the PMS 1003 sensors had a housing but no difference when the housing was removed (Fig. S-6). The effect of the housing appears to be less important for winter-time ambient conditions (Fig. 3a, a median mass-based particle size of 0.40 μm, mass basis estimated by GRIMM, assuming an average particle density of 2 g/cm^3) than for the wind-tunnel tests (median particle size of 3.5 μm, mass basis estimated by GRIMM). However, we have limited results, and this requires additional investigation.

The slope of the linear relationship between the PMS (y) sensor and mass adjusted DustTrack (x) ranges from 0.17 to 0.25 m^3/μg. This differs by a factor of five compared to the slope for the ambient data (PMS (y) and TEOM (x) of 1.26 m^3/μg (full ambient concentration range) and PMS (y) and TEOM (x) of 1.81 m^3/μg (up to 40 μg/m^3)). By way of comparison, the slope for the GRIMM in the wind tunnel is 0.65 m^3/μg (GRIMM (y) and DustTrack (x)) compared to the ambient environment slope of 0.47 m^3/μg (GRIMM (y) and

TEOM (x)). The SQAMD reports a slope ranging from 1.35 to 1.50 m^3/μg (FEM (x) and PMS 1003 (y)) for their ambient comparisons (SCAQMD, 2016). This emphasizes the likely importance of particle properties in the response of the PMS sensor. Austin et al. (2015) reported that the slope of the linear relationship between a Shinyei sensor and an APS varied by a factor of 10 depending on particle diameter. In general, the performance of inexpensive sensors can differ markedly in the field compared to laboratory validations (Piedrahita et al., 2014). It is unclear why the PMS's is much more sensitive to CAP particles compared to the GRIMM, but it is possible that the causes are related to particle size and composition as well as the differences in sensor optics and how the sensors transform the detected laser signals into particle concentration. Both the PMS and GRIMM measure light scattering at approximately 650 nm, and Mie scattering reaches its peak for particles with diameters in the range of 300–700 nm, at a wavelength of 400–700 nm (Finlayson-Pitts and Pitts, 2000). During CAPs, particles, due the large contributions of secondary aerosols, likely have a large scattering efficiency, and particle mass distributions exhibit a peak in the range of 300–500 nm (Fig. S-4). In addition, particles entering the PMS sensor must make three 90-degree turns before passing the laser. The larger particle sizes in the wind-tunnel tests likely do not reach the laser as readily as the smaller CAP particles.

### 3.3.2. Particle counts and size distributions

In the wind-tunnel experiments, the PMS sensors generally capture the particle size distribution compared to the GRIMM. They

Table 2
Summary of R^2 values for the wind-tunnel tests. The number of average 10-min averages used to generate the is included in parentheses.

RSQ	DT Adj	GRIMM	PMS 3003-1	PMS 3003-2	PMS 1003-1	PMS 1003-2	Shinyei1	Shinyei3
DT adj	1	(11,16)	(11,8)	(16,8)	(16,16)	(16,16)	(16,16)	(8,16)
GRIMM	0.80,0.97	1	(11,8)	(11,8)	(11,16)	(11,16)	(11,16)	(8,16)
PMS 3003-1	0.92,0.95	0.80, 0.94	1	(11,8)	(11,8)	(11,8)	(11,8)	(8,8)
PMS 3003-2	0.83,0.97	0.73, 0.97	0.88, nd	1	(16,0)	(16,8)	(16,8)	(8,8)
PMS 1003-1	0.92, 0.98	0.93, 0.98	0.95,0.97	0.82,0.99	1	(11,8)	(11,8)	(8,8)
PMS 1003-2	0.89, 0.96	0.69, 0.99	0.95,0.97	0.95, 0.99	0.88, 0.99	1	(16,8)	(8,8)
Shinyei1	0.68, 0.80	0.60,0.71	0.80, 0.99	0.81, 0.97	0.63, 0.77	0.58, 0.77	1	(8,16)
Shinyei3	0.59, 0.62	0.50, 0.73	0.50, 0.98	0.64, 0.98	0.55, 0.65	0.49, 0.56	0.72, 0.95	1

Nd: no data.
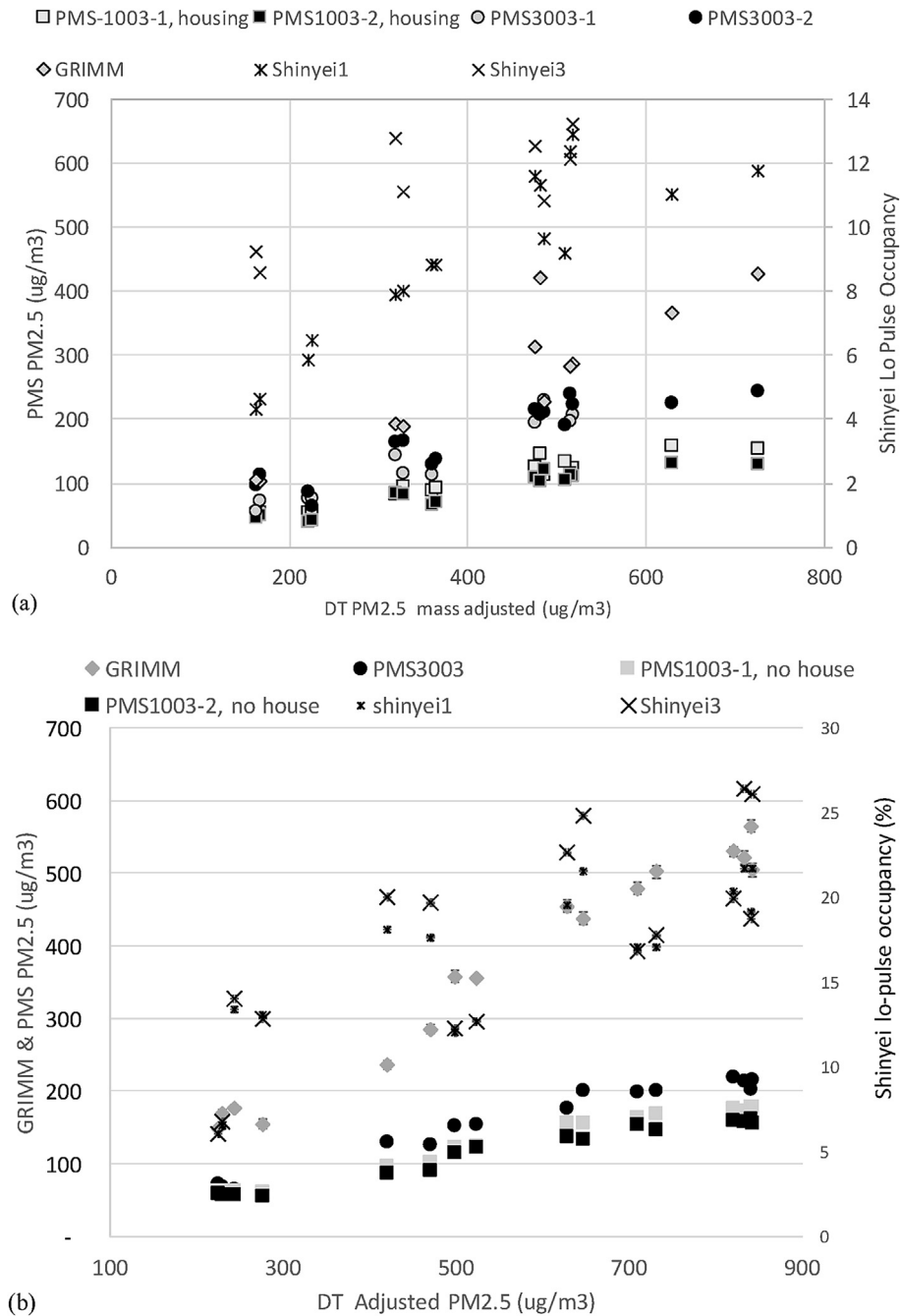
Fig. 6. Ten-minute average PM$_{2.5}$ concentration and lo-occupancy percentage (Shinyei) versus DustTrack mass-adjusted PM$_{2.5}$ concentration with standard errors shown. Each point is the summary of four average measurements at each wind-tunnel condition. Fig. 6a shows the PMS 1003 sensor response with a housing, and Fig. 6b shows a subsequent experiment with the housing removed from the PMS 1003s. In Fig. 6b, the PMS 3003 sensor readings are combined because they do not overlap.

also underestimate particle counts by a factor of 80% or more compared to the GRIMM for PM smaller than 10 μm in diameter but slightly overestimates particle counts compared to the GRIMM at the 10 μm size bin, by a factor of 2.5 (Fig. S-7 and S-8). The median particle size measured by the GRIMM is 0.33 μm (count basis) and 3.5 μm (mass basis), and the median particle size measured by the PMS sensors was 0.3 μm (count basis) and 6 μm (mass basis). For the APS, the median particle size is 1.15 μm (count basis) and 4.99 μm (mass basis). The difference in count-based median particle size between the APS and the GRIMM or PMS is likely due to the inability of the APS to "see" particles smaller than 0.523 μm. The median particle size of the alumina oxide particles is 4.9 μm (mass basis, reported by manufacturer), close to the APS's estimated

median particle size (mass basis). Just as with the mass measurements, the PMS sensors underestimate particle counts in the wind-tunnel compared to the ambient environment where they overestimate particle counts.

4. Conclusions

This study demonstrated that the PMS 1003/3003 correlates well with FRMs, FEMs, and research-grade instrumentation under ambient conditions during a series of CAPs and in a wind-tunnel environment. Under ambient conditions, this sensor correlates better with a FRM than other low-cost sensors in similar studies. However additional measurements are needed under a variety of

ambient conditions to adequately compare the performance of low-cost PM sensors. Although the PMS correlates well to FRMs, it overestimates PM concentration during CAPs, which has important implications for communication of the results to the public as well as for other regions of the world that suffer from periodic episodes of high PM concentration associated with CAPs and with large contributions from secondary aerosols. Furthermore, its response to PM concentration varies with particle properties to a much greater degree than research-grade instrumentation. In addition, we identified potential interference caused by the sensor housing developed by the community organization. These results highlight the importance of evaluating the sensor under the target conditions and developing an appropriate correction factor if the user wants to compare low-cost sensor results to FEM/FRMs. In spite of these challenges, these sensors are a promising tool for identifying relative increases or decreases in PM concentration, complementing sparsely distributed monitoring stations and for assessing and minimizing exposure to PM.

Acknowledgments

Appendix A. Supplementary data

Supplementary data related to this article can be found at http://dx.doi.org/10.1016/j.envpol.2016.12.039.

References

Afsarmanesh, N., 2013. Smog blog: world-class pollution brings Tehran to a halt. Sci. Am. March 2, 2013 https://blogs.scientificamerican.com/observations/smog-blog-world-class-pollution-brings-tehran-to-a-halt/.

Austin, E., Novosselov, I., Seto, E., Yost, M.G., 2015. Laboratory evaluation of the Shinyei PPD42NS low-cost particulate matter sensor. PLoS One 10, e0137789.

Beard, J.D., Beck, C., Graham, R., Packham, S.C., Traphagan, M., Giles, R.T., Morgan, J.G., 2012. Winter temperature inversions and emergency department visits for asthma in Salt Lake County, Utah, 2003-2008. Environ. Health Perspect. 120, 1385–1390. http://dx.doi.org/10.1289/ehp.1104349.

Bell, M.L., Ebisu, K., Peng, R.D., 2011. Community-level spatial heterogeneity of chemical constituent levels of fine particulates and implications for epidemiological research. J. Expo. Sci. Env. Epidemiol. 21, 372–384.

Bischoff, P., n.d. New gadget precisely gauges indoor air pollution and finds places with clean air nearby. TechInAsia.

Brook, R.D., Rajagopalan, S., Pope, C.A., Brook, J.R., Bhatnagar, A., Diez-Roux, A.V., Holguin, F., Hong, Y., Luepker, R.V., Mittleman, M.A., Peters, A., Siscovick, D., Smith, S.C., Whitsel, L., Kaufman, J.D., 2010. Particulate matter air pollution and cardiovascular disease: an update to the scientific statement from the american heart association. Circulation 121, 2331–2378. http://dx.doi.org/10.1161/CIR.0b013e3181dbece1.

Brookings Institute, 2012. Mountain Megas: a Profile of Utah's Wasatch Front. Washington, DC.

Chow, J.C., Watson, J.G., Lowenthal, D.H., Richards, L.W., 2002. Comparability between PM2.5 and particle light scattering measurements. Environ. Monit. Assess 79, 29–45.

DAQ (Utah Division of Air Quality), 2013. State Implementation Plan, Subsection IX.A.21: Control Measures for Area and Point Sources, Fine Particulate Matter, PM2.5 SIP for the Salt Lake City. UT Nonattainment Area, Salt Lake City, UT.

EPA, 2009. Integrated Science Assessment for Particulate Matter. Research Triangle Park.

Finlayson-Pitts, B.J., Pitts, J.N.J., 2000. Upper and Lower Atmosphere. AP Academic Press, London, UK.

Gao, M., Cao, J., Seto, E., 2015. A distributed network of low-cost continuous reading sensors to measure spatiotemporal variations of PM2.5 in Xi'an, China. Environ. Pollut. 199, 56–65. http://dx.doi.org/10.1016/j.envpol.2015.01.013.

Health Effects Institute, 2010. Traffic-related Air Pollution: a Critical Review of the Literature on Emissions, Exposure, and Health Effects.

Holstius, D.M., Pillarisetti, A., Smith, K.R., Seto, E., 2014. Field calibrations of a low-cost aerosol sensor at a regulatory monitoring site in California. Atmos. Meas. Tech. 7, 1121–1131. http://dx.doi.org/10.5194/amt-7-1121-2014.

Isaac, M., 2014. Regulatory considerations of lower cost air pollution sensor data performance. Environ. Manage 7, 32–37. http://dx.doi.org/10.1016/B978-0-12-385485-8.00002-5.

Kaiser, H., Specker, H., 1956. Bewertung und Vergleich von Analysenverfahren. Fresenius' J. Anal. Chem. 149, 46–66.

Kelly, K.E., Kotchenruther, R., Kuprov, R., Silcox, G.D., 2013. Receptor model source attributions for Utah's Salt Lake City airshed and the impacts of wintertime secondary ammonium nitrate and ammonium chloride aerosol. J. Air Waste Manage. Assoc. 63, 575–590. http://dx.doi.org/10.1080/10962247.2013.774819.

Kulkarni, P., Baron, P., Willeke, K., 2011. Aerosol Measurement: Principles, Techniques, and Applications, third ed. John Wiley & Sons, Ltd.

Lepeule, J., Laden, F., Dockery, D., Schwartz, J., 2012. Chronic exposure to fine particles and mortality: an extended follow-up of the Harvard six cities study from 1974 to 2009. Environ. Health Perspect. 120, 965–970. http://dx.doi.org/10.1289/ehp.1104660.

Lewis, A., 2016. Validate personal air-pollution sensors. Nature 535, 29–31.

Molina, L.T., Kolb, C.E., de Foy, B., Lamb, B.K., Brune, W.H., Jimenez, J.L., Molina, M.J., 2007. Air quality in North America's most populous city: an overview of MCMA-2003 Campaign. Atmos. Chem. Phys. Discuss. 7, 3113–3177. http://dx.doi.org/10.5194/acpd-7-3113-2007.

Murphy, D.M., Cziczo, D.J., Hudson, P.K., Schein, M.E., Thomson, D.S., 2004. Particle density inferred from simultaneous optical and aerodynamic diameters sorted by composition. J. Aerosol Sci. 35, 135–139.

Peters, A., Liu, E., Verrier, R.L., Schwartz, J., Gold, D.R., Mittleman, M., Baliff, J., Oh, J.A., Allen, G., Monahan, K., Dockery, D.W., 2000. Air pollution and incidence of cardiac arrhythmia. Epidemiology 11.

Peters, T.M., Ott, D., O'Shaughnessy, P.T., 2006. Comparison of the Grimm 1.108 and 1.109 portable aerosol spectrometer to the TSI 3321 aerodynamic particle sizer for dry particles. Ann. Occup. Hyg. 50, 843–850. http://dx.doi.org/10.1093/annhyg/mel067.

Piedrahita, R., Xiang, Y., Masson, N., Ortega, J., Collier, A., Jiang, Y., Li, K., Dick, R.P., Lv, Q., Hannigan, M., Shang, L., 2014. The next generation of low-cost personal air quality sensors for quantitative exposure monitoring. Atmos. Meas. Tech. 7, 3325–3336. http://dx.doi.org/10.5194/amt-7-3325-2014.

Pope, C.A., Burnett, R.T., Thun, M.J., Calle, E.E., Krewski, D., Ito, K., Thurston, G.D., 2002. Lung cancer, cardiopulmonary mortality, and long-term exposure to fine particulate air pollution. J. Am. Med. Assoc. 287.

Pope, A.C., Burnett, R.T., Turner, M.C., Cohen, A., Krewski, D., Jerrett, M., Gapstur, S.M., Thun, M.J., 2011. Lung cancer and cardiovascular disease mortality associated with ambient air pollution and cigarette smoke: shape of the exposure-response relationships. Environ. Health Perspect. 119, 1616–1621. http://dx.doi.org/10.1289/ehp.1103639.

PurpleAir, 2016. PurpleAir Air Quality Map. Accessed 2016-06-06 [WWW Document]. URL. http://map.purpleair.org/. https://script.google.com/macros/s/AKfycbwzxhzw9IXNugu-A0lpcos7meQnBm9YEuVPxyPO21Q8ow6xlp0/exec. accessed 1.1.16.

SCAQMD, 2016. Draft: Field Evaluation PurpleAir PM Sensor.

Schmees, D.K., Wu, Y.-H., Vincent, J.H., 2008. Experimental methods to determine inhalability and personal sampler performance for aerosols in ultra-low windspeed environments. J. Environ. Monit. 10, 1426–1436. http://dx.doi.org/10.1039/b806431h.

Schubert, E., 2006. Light-Emitting Diodes. Cambridge University Press, Cambridge, UK.

Steinle, S., Reis, S., Sabel, C.E., 2013. Quantifying human exposure to air pollution–moving from static monitoring to spatio-temporally resolved personal exposure assessment. Sci. Total Environ. 443, 184–193. http://dx.doi.org/10.1016/j.scitotenv.2012.10.098.

US Department of Commerce, 2010. US 2010 Census. Washington, DC.

USEPA, 1999. Ambient Air Monitoring Reference and Equivalent Methods. USA.

Wang, Y., Li, J., Jing, H., Zhang, Q., Jiang, J., Biswas, P., 2015. Laboratory evaluation and calibration of three low-cost particle sensors for particulate matter measurement. Aerosol Sci. Technol. 49, 1063–1077. http://dx.doi.org/10.1080/02786826.2015.1100710.

Watson, J.G., Chow, J.C., 2002. A wintertime PM2.5 episode at the Fresno, CA, supersite. Atmos. Environ. 36, 465–475. http://dx.doi.org/10.1016/S1352-2310(01)00309-0.

Whiteman, C.D., Hoch, S.W., Horel, J.D., Charland, A., 2014. Relationship between particulate air pollution and meteorological variables in Utah's Salt Lake Valley. Atmos. Environ. 94, 742–753. http://dx.doi.org/10.1016/j.atmosenv.2014.06.012.

World Health Organization, 2014. Burden of Disease from Ambient Air Pollution for 2012.

Zeft, A.S., Prahalad, S., Lefevre, S., Clifford, B., Mcnally, B., Bohnsack, J.F., Pope, C.A., 2009. Juvenile idiopathic arthritis and exposure to fine particulate air pollution. Clin. Exp. Rheumatol. 27, 877–884.

Zhang, Y.-L., Cao, F., 2015. Fine particulate matter (PM2.5) in China at a city level. Sci. Rep. 5, 14884. http://dx.doi.org/10.1038/srep14884.